

1 This document is the Accepted Manuscript version of a
2 Published Work that appeared in final form in *Canadian*
3 *Journal of Chemistry*, copyright © Canadian Science
4 Publishing, after peer review and technical editing by the
5 publisher.

6
7 To access the final edited and published work see

8
9 *Canadian Journal of Chemistry* **2021**, 99, 245-252

10
11 <https://doi-org.uml.idm.oclc.org/10.1139/cjc-2020-0333>

12
13 Also see same web-link for Supporting Information,
14 available free of charge.

15

16 Synthesis, Characterization and Coordination
17 Chemistry of a Phenanthridine-Containing *N*-
18 Heterocyclic Carbene Ligand

19

20 Rajarshi Mondal, Robert J. Ortiz, Jason D. Braun and David E. Herbert*

21

22

23 Department of Chemistry and the Manitoba Institute for Materials, University of Manitoba, 144
24 Dysart Road, Winnipeg, Manitoba, R3T 2N2, Canada

25

26 *david.herbert@umanitoba.ca

27

28

29

30 ABSTRACT

31 An *N*-heterocyclic carbene ligand precursor bearing a π -extended phenanthridine (3,4-
32 benzoquinoline) unit is presented. The proligand was isolated as the imidazolium salt of chloride
33 (**1**•HCl), bromide (**1**•HBr) or hexafluorophosphate (**1**•HPF₆) counterions. These salts can be
34 deprotonated and the carbene installed on silver centres using Ag₂O as both a base and a source of
35 metal ion. The resulting Ag(I) complex (**1**)AgCl can be used in a transmetalation reaction to
36 generate a Pd(II) coordination complex (**1**)Pd(CH₃CN)Cl₂. The characterization and photophysical
37 properties of these complexes is presented, along with a demonstration of the utility of
38 (**1**)Pd(CH₃CN)Cl₂ in mediating a catalytic C-N cross-coupling reaction for the preparation of the
39 pharmaceutical Piribedil.

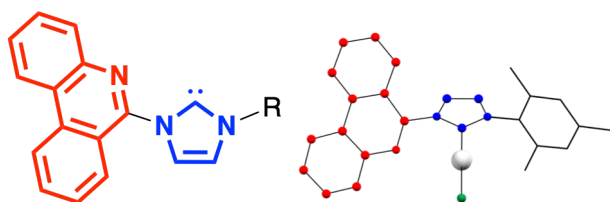
40

41 Keywords

42 *N*-heterocyclic carbenes, phenanthridine, ligand design, transmetalation, piribedil

43

44 Table of Contents Graphic

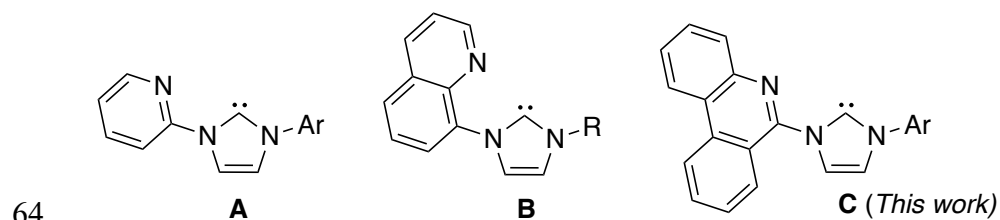


45 ***Phenanthridine-Carbene Hybrid Ligands***

46

47 **INTRODUCTION**

48 *N*-Heterocyclic carbenes (NHCs) are a well-established and versatile class of ligand in
49 coordination chemistry,¹ known mainly as strong σ -donors, but with widely tunable steric and
50 electronic properties.² In addition to myriad monodentate variants, NHCs have also been used as
51 part of multidentate ligand scaffolds, paired with both neutral³ and anionic⁴ tethers in order to
52 chelate both softer and harder metals. Morris and coworkers have developed this concept to great
53 success over the years, preparing nitrile⁵ and primary amine-functionalized^{6,7} NHCs which form
54 late transition metal complexes that can serve as active catalysts for the hydrogenation of polar
55 molecules such as imines,⁸ esters^{8,9} and ketones.^{7,10,11} In such systems, the NHC ligand is thought
56 to balance the hydricity of metal hydride intermediates and the acidity of the tethered NH group,
57 enhancing their reactivity in transfer hydrogenation.¹² In addition, where inner-sphere mechanisms
58 involving hemilability of the amine arm have been proposed, the strong NHC donor helps anchor
59 the ligand framework to the metal centre, facilitating bifunctional reactivity.¹³ Other ancillary
60 ligands that have been combined with NHCs into multidentate scaffolds include π -accepting *N*-
61 heterocycles such as pyridines,^{14,15} quinolines,^{16–18} pyrimidines¹⁹ and phenanthrolines²⁰ (Figure 1).
62 These form hybrid push-pull type ligands that can also be used to access bifunctionality and
63 hemilability,²¹ as well as complexes with variable electronic structures.^{22,23}



65 **Figure 1.** Selected examples of (benzannulated) pyridine-tethered *N*-heterocyclic carbenes (**A**¹⁴,
66 **C** (this work): Ar = 2,4,6-trimethylphenyl (mesityl); **B**¹⁸: R = *n*Pr).

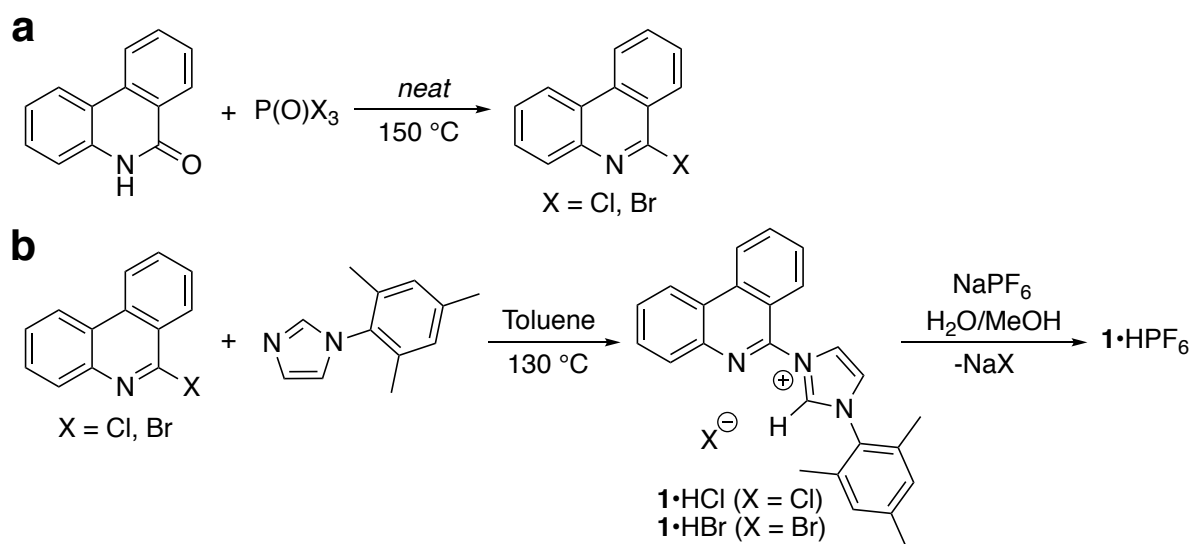
67 We have been exploring pairing π -extended *N*-heterocycles such as phenanthridine (3,4-
68 benzoquinoline) with phosphines²⁴ and amines²⁵ in ditopic P^N and N^N scaffolds, as well as in
69 pincer-type tridentate N^N^N proligands in combination with amido donors and either a tertiary
70 amine²⁶ or second heterocyclic arm.²⁷ Compared with pyridine, quinoline and phenanthroline, the
71 coordination chemistry of phenanthridine as part of multidentate ligand frameworks or even on its
72 own^{28–32} is considerably underexplored. Given the exceptional properties of carbene donors, we
73 decided to pursue a C^N variant wherein a phenanthridine heterocycle was tethered to an NHC
74 donor arm. In such analogs (**C**), the chelate size as well as the site of benzannulation compared
75 with known *N*-heterocyclic/NHC systems (e.g., **A–B**) would be changed, with potential
76 implications for the electronic and materials properties,³³ and reactivity of its complexes.¹³

77

78 RESULTS AND DISCUSSION

79 A phenanthridine-tethered *N*-heterocyclic carbene was targeted in the form of the protonated
80 imidazolium, as a salt of chloride (**1**•HCl), bromide (**1**•HBr) and hexafluorophosphate (**1**•HPF₆)
81 counterions. Imidazoliums **1**•HCl and **1**•HBr were prepared by *N*-arylation of an *N*-substituted
82 imidazole with 6-chlorophenanthridine³⁴ or 6-bromophenanthridine, respectively. The
83 halogenated phenanthridines were accessed in appreciable yields (62% and 84%, respectively) as
84 light yellow solids via reaction of 6-(5*H*)-phenanthridinone³⁵ with the appropriate phosphorus(V)
85 oxyhalide (POX₃; X = Cl, Br) at 150 °C (Scheme 1a). Reaction of either 6-halophenanthridine
86 with 1-mesityl-1*H*-imidazole (mesityl = 2,4,6-trimethylphenyl) in refluxing toluene yielded **1**•HCl
87 (81%) and **1**•HBr (85%) as off-white solids (Scheme 1b). ¹H NMR spectra of both products
88 contained a downfield singlet attributable to the acidic imidazolium *CH* nucleus, diagnostic of
89 each salt [δ_{H} : 10.36 ppm (**1**•HCl), 10.62 ppm (**1**•HBr)]. This was accompanied by a similarly

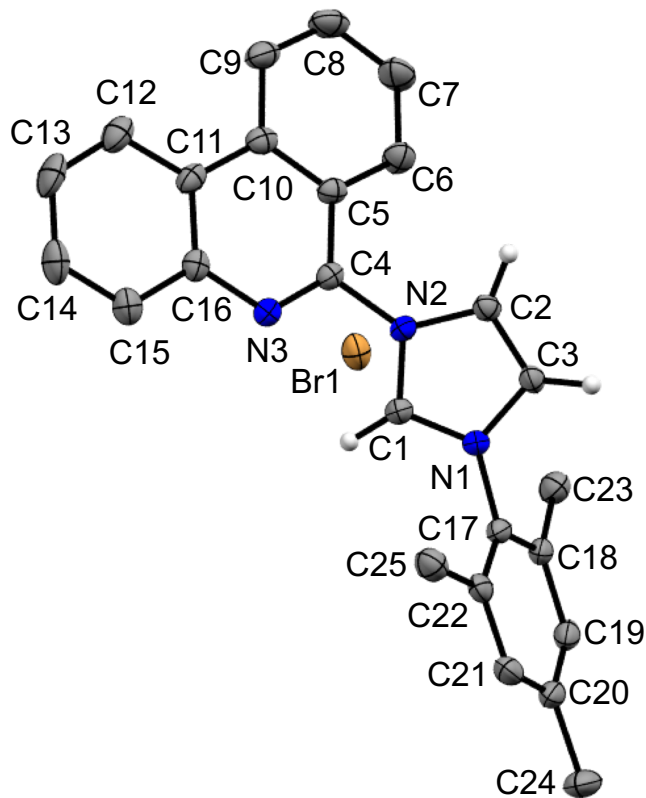
90 deshielded signal in the $^{13}\text{C}\{^1\text{H}\}$ NMR spectrum [$\delta_{\text{C}} = 145.5$ ppm ($\mathbf{1}\cdot\text{HCl}$), 144.6 ($\mathbf{1}\cdot\text{HBr}$)]
 91 attributed to the attached carbon. To improve solubility in organic solvents, a hexafluorophosphate
 92 analog ($\mathbf{1}\cdot\text{HPF}_6$) was prepared via salt metathesis of $\mathbf{1}\cdot\text{HCl}$ with NaPF_6 in a water/methanol
 93 mixture. The NMR spectra of all three salts also show additional resonances in the aromatic region
 94 assigned to the phenanthridinyl unit. Notably, a diagnostic singlet resonance attributable to a
 95 hydrogen nucleus in the 6-position of the phenanthridinyl units³⁶ was absent, confirming
 96 attachment of the *N*-heterocycle at this position.



98 **Scheme 1.** Synthesis of (a) (6-chloro/bromo)phenanthridine and (b) phenanthridine-tethered
 99 imidazoliums $\mathbf{1}\cdot\text{HCl}$, $\mathbf{1}\cdot\text{HBr}$ and $\mathbf{1}\cdot\text{HPF}_6$.

100 To confirm the structure assigned in solution, single crystals of a representative analog ($\mathbf{1}\cdot\text{HBr}$)
 101 were grown from a mixture of hexanes-dichloromethane and analyzed by X-ray diffraction. The
 102 solid-state structure confirms the installation of the 1-mesitylimidazole at the 6-position of the
 103 phenanthridine unit, along the presence of a bromide counterion (Figure 2). A slightly shorter C=N
 104 distance is observed in the phenanthridinyl unit [C(13)-N(1) 1.286(4) Å] when compared to other
 105 reported phenanthridine-based proligands^{37,38} in which the 6-position of remains unsubstituted

106 [d(C=N) ~1.3-1.31 Å]. The remainder of the bond lengths and angles in both the NHC and
107 phenanthridinyl unit are otherwise unremarkable.

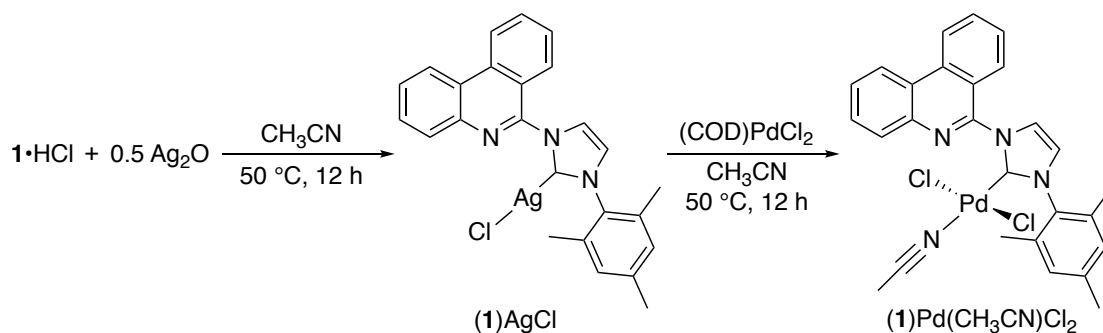


108
109 **Figure 2.** Solid-state structure of **1**•HBr with thermal ellipsoids shown at 50% probability levels.
110 A molecule of the crystallization solvent (CH₂Cl₂), select hydrogen atoms and labels have been
111 omitted for clarity. Selected bond distances (Å) and angles (°): C1-N2 1.338(4), C1-N1 1.321(4),
112 C2-N2 1.390(4), C3-N1 1.386(4), C4-N2 1.436(4), C17-N1 1.454(4), C4-N3 1.286(4), C4-C5
113 1.436(4); N3-C4-N2 113.9(3), N1-C1-N2 108.4(3), C3-C2-N2 107.0(3), C2-C3-N1 107.2(3),
114 C22-C17-N1 118.4(3), N3-C4-C5 126.4(3), C4-N3-C16 118.2(3), C1-N2-C2 108.4(3), C1-N2-C4
115 122.9(3), C2-N2-C4 128.4(3), C1-N1-C3 109.0(3), C1-N1-C17 126.2(3), C3-N1-C17 124.7(3).

116

117 **Coordination Chemistry of 1**

118 To explore the coordinating ability of tethered phenanthridinyl-carbenes derived from **1**•HX, we
119 first prepared a Ag(I) complex (Scheme 2). Linear Ag(I)-NHC complexes are capable of
120 transmetalation reactions and thus are useful sources of carbene ligands.³⁹ To install our hybrid
121 carbene ligand on Ag(I), **1**•HCl was reacted with Ag₂O in acetonitrile at 50°C to provide both a
122 Brønsted base for deprotonation of the imidazolium and a source of silver. The resultant
123 suspension was filtered over Celite and repeatedly precipitated from diethylether/dichloromethane
124 to yield (**1**)AgCl as a white solid. The ¹H NMR spectrum of (**1**)AgCl revealed the absence of a
125 signal attributable to the imidazolium CH of **1**•HCl, which supports installation of **1** on a Ag(I)
126 centre in its deprotonated carbene form, though the carbene resonance could not be observed by
127 ¹³C NMR spectroscopy. Signals for carbene carbon nuclei in linear NHC silver halide complexes
128 have been reported over a wide ppm range (213.7-163.2 ppm).⁴⁰ The appearance of these
129 resonances can be concentration-dependent, and in some cases, absent completely,⁴¹⁻⁴³ as is the
130 case for (**1**)AgCl. High-resolution electrospray ionization mass spectrometry (HR ESI-MS)
131 confirmed ligation of **1**, with peaks consistent with (**1**)AgCl, as well as an ion formed by loss of
132 the chloride. The major peak, however, belongs to the *bis*-NHC cation [(**1**)₂Ag]⁺ (Figure S1). This
133 is consistent with literature reports that NHC silver halide complexes form *bis*(carbenes) in the gas
134 phase.⁴⁰

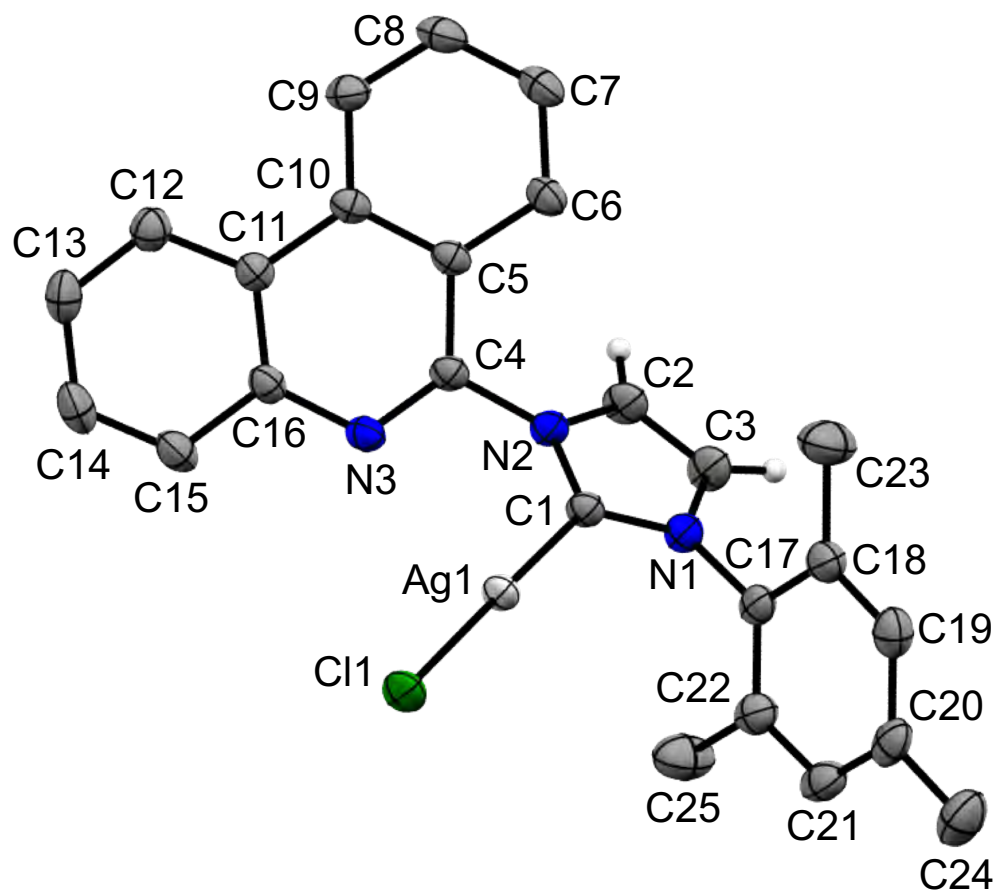


135

136 **Scheme 2.** Synthesis of coordination complexes (**1**)AgCl and (**1**)Pd(CH₃CN)Cl₂.

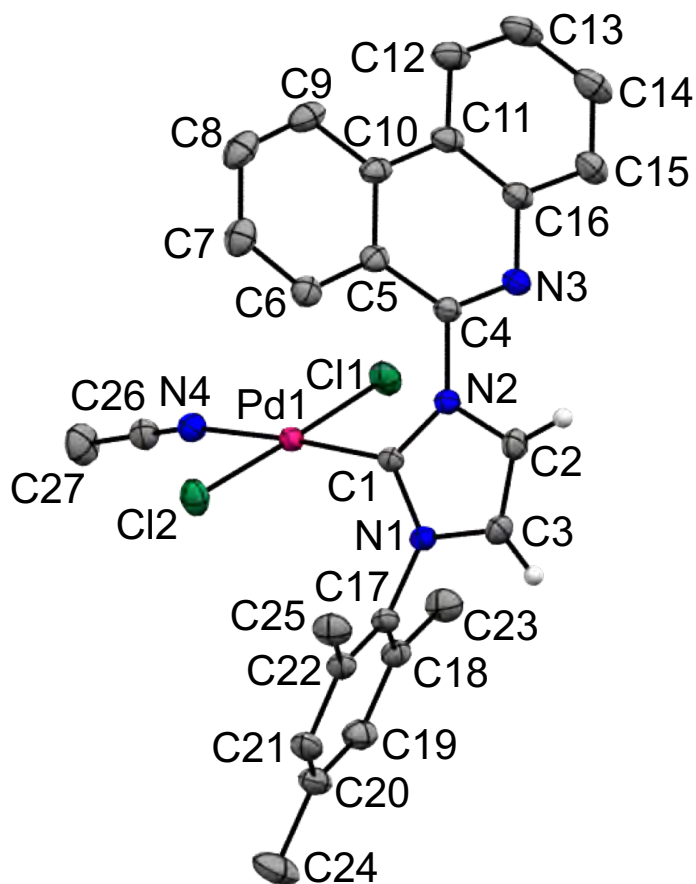
137 To confirm the structure assigned in solution, a single crystal of (**1**)AgCl was similarly analyzed
138 by X-ray diffraction (Figure 3). Suitable crystals were grown by diffusion of hexane vapours into
139 a dichloromethane solution at -10°C. In the solid-state, a linear geometry around the Ag(I) centre
140 can be seen [C1-Ag1-Cl1 angle of 177.68(6)°] with coordination of both the NHC of **1** and a
141 chloride. The phenanthridinyl arm remains pendent and uncoordinated to silver (N3---Ag1 ~ 3.23
142 Å). While this separation is just within the sum of the van der Waals radii (3.27 Å),⁴⁴ the
143 phenanthridine nitrogen (N3) is not oriented towards the Ag centre and the phenanthridine ring
144 system is twisted relative to the plane of the NHC moiety [50.6° *cf.* 41.8° in **1**•HBr]. The
145 phenanthridinyl arm, in fact, shows a closer hydrogen bonding interaction with co-crystallized
146 CH₂Cl₂ (N3-H26A 2.470 Å; N3-H26A-C26 157.98°). A close C1-Ag1 interaction of 2.0689(19)
147 Å is present, along with a Ag1-Cl1 bond length of 2.3232(5) Å, in range of values reported for
148 similar complexes.⁴⁵⁻⁴⁷ The angle about the carbene carbon internal to the NHC is constricted
149 compared to in **1**•HBr [N1-C1-N2: 104.39(16)° vs 108.4(3)° in **1**•HBr], with a slight increase in
150 the corresponding C-N bonds [C1-N2 1.360(2), C1-N1 1.346(3) Å; *cf.* C1-N2 1.338(4), C1-N1
151 1.321(4) Å in **1**•HBr].

152



153
 154 **Figure 3.** Solid-state structure of (1)AgCl with thermal ellipsoids shown at 50% probability levels.
 155 A molecule of the crystallization solvent (CH₂Cl₂), select hydrogen atoms and labels are omitted
 156 for clarity. Selected bond distances (Å) and angles (°): Ag1-C1 2.0689(19), Ag1-Cl1 2.3232(5),
 157 C4-N3 1.289(3), C4-N2 1.433(3), C16-N3 1.385(3), C1-N2 1.360(2), C1-N1 1.346(3), C3-N1
 158 1.385(3), C2-N2 1.393(3), C2-C3 1.336(3), C17-N1 1.441(3); C1-Ag1-Cl1 177.68(6), N3-C4-C5
 159 125.92(19), N3-C4-N2 115.74(17), N2-C4-C5 118.33(17), N1-C1-N2 104.39(16), N2-C1-Ag1
 160 127.97(14), N1-C1-Ag1 127.18(14), C4-N3-C16 117.73(17), C1-N2-C4 123.28(16), C1-N2-C2
 161 110.69(17), C2-N2-C4 125.93(17), C1-N1-C3 111.36(18), C1-N1-C17 123.02(17), C3-N1-C17
 162 125.08(18).

163 The silver complex can be used to transmetalate **1** to other transition metal centres. A palladium
164 coordination complex was accordingly prepared by reaction of (**1**)AgCl with (COD)PdCl₂ (COD
165 = 1,5-cyclooctadiene) in acetonitrile at ambient temperature. The resulting yellow solid could in
166 fact be purified by column chromatography on silica (1:1 CH₃CN:Et₂O eluent; 37% yield),
167 highlighting the strong σ -bonding of **1** to Pd. The ¹H NMR spectra of the complex showed
168 retention of the phenanthridine-tethered carbene ligand but also a singlet corresponding to an
169 equivalent of CH₃CN, used as the solvent for synthesis, in the coordination sphere of palladium (δ
170 = 2.00 ppm; δ (free CH₃CN) = 2.10 ppm⁴⁸). Anticipating monodentate binding of **1** and retention
171 of both chlorides, the structure of the Pd(II) complex was therefore formulated as
172 (**1**)Pd(CH₃CN)Cl₂. A distorted square-planar geometry was verified in solid-state (Figure 4), with
173 the expected range of bond angles about the metal centre between *cis*-disposed ligands (~88-93°)
174 and a nearly linear C11-Pd1-Cl2 angle of 178.49(2)°. The C_{NHC}-Pd-N_{CH₃CN} angle is slightly acute
175 in comparison [C1-Pd1-N4 173.89(7)°]. The bond length between C1-Pd1 is measured to be
176 1.953(2) Å, within error of closely related carbene dichloride palladium(II) pyridine complexes.⁴⁹
177 Befitting the uncoordinated phenanthridine, the twist between the pendent *N*-heterocycle and the
178 plane of the NHC is increased further to 62.95°, with a N_{phenanthridine}---Pd separation of 4.323 Å,
179 well outside the sum of the Van der Waals radii (3.18 Å).⁴⁴ The *trans* influence displayed by the
180 NHC in (**1**)Pd(CH₃CN)Cl₂ [C1-Pd1 1.9532(18) Å; N4-Pd1 2.0642(17) Å] is consistent with other
181 NHC ligands in analogous palladium complexes containing a *trans*-disposed acetonitrile and two
182 *cis* chlorides, evinced by both comparable C_{NHC}-Pd (1.939-1.976 Å) and *trans* Pd-N_{CH₃CN} bond
183 lengths (2.066-2.092 Å).⁵⁰⁻⁵⁵



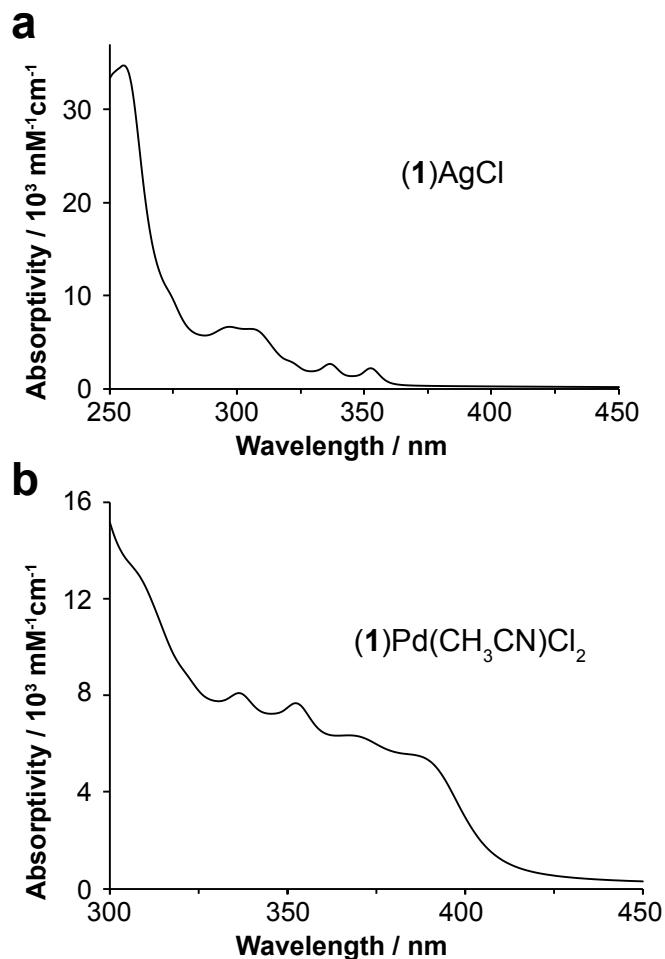
184

185 **Figure 4.** Solid-state structure of (1)Pd(CH₃CN)Cl₂ with thermal ellipsoids shown at 50%
 186 probability levels. Selected bond distances (Å) and angles (°): C11-Pd1 2.2885(5), Cl2-Pd1
 187 2.3095(5), N4-Pd1 2.0642(17), C1-Pd1 1.9532(18), C1-N2 1.357(2), C1-N1 1.350(2), C2-N2
 188 1.391(2), C3-N1 1.391(2), C4-N3 1.291(3), C4-N2 1.442(2), C16-N3 1.387(2), C17-N1 1.440(2);
 189 N1-C1-N2 105.03(15), N1-C1-Pd1 125.13(13), N2-C1-Pd1 129.51(13), C3-C2-N2 106.45(16),
 190 N3-C4-C5 126.64(18), N3-C4-N2 114.09(17), C5-C4-N2 119.27(17), N3-C16-C15 116.74(19),
 191 N3-C16-C11 122.48(19), C26-N4-Pd1 167.33(18), C1-Pd1-N4 173.89(7), C1-Pd1-Cl1 87.75(5),
 192 N4-Pd1-Cl1 89.87(5), C1-Pd1-Cl2 93.04(5), N4-Pd1-Cl2 89.47(5), Cl1-Pd1-Cl2 178.49(2).

193 Absorption spectra of (1)AgCl and (1)Pd(CH₃CN)Cl₂ were collected to explore the electronic
 194 structures of these complexes. The Ag(I) complex is a d¹⁰ system and isoelectronic with

195 phenanthridine-based *P*[^]*N* ligated Cu(I) complexes that have been previously reported.⁵⁶ The
196 electronic absorption spectrum of (**1**)AgCl (Figure 5a) is in fact quite similar to those of the Cu(I)
197 complexes, with peaks in the UV region at ~250-300 nm and a weak tail at ~350 nm nearing the
198 visible. The lowest energy absorption of (**1**)AgCl displays solvatochromism, with a hypsochromic
199 shift observed upon increasing solvent polarity (Figure S2) consistent with n- π^* character to this
200 absorption.⁵⁷ The solvatochromic trend breaks down in methanol, likely as a result of solvent-
201 induced displacement of the chloride. The silver complex is also weakly fluorescent in solution
202 ($\lambda_{em} = 373$ nm; $\phi = 0.04$ vs quinine sulfate; Figure S3). In comparison, the aforementioned Cu(I)
203 analogs are phosphorescent.⁵⁶ There, the phenanthridine unit is bound to the transition metal
204 element and the resultant complexes emit from triplet states due to intersystem crossing assisted
205 by the presence of the Cu nuclei. Here, the emission originates from the uncoordinated
206 phenanthridinyl arm. Installation of **1** on a d⁸ metal centre such as Pd(II) introduces higher energy
207 filled orbitals capable of engaging transitions that are metal-ligand charge-transfer (MLCT) in
208 character. Accordingly, in the UV-Vis absorption spectrum of (**1**)Pd(CH₃CN)Cl₂, lower energy
209 peaks at 367 and 388 nm are observed alongside the peaks at ~350 nm also observed in the
210 spectrum of (**1**)AgCl (Figure 5b). This explains the light yellow colour to the Pd(II) complex
211 compared to (**1**)AgCl, which was isolated as a white solid.

212



213

214 **Figure 5.** UV-Vis absorption spectra of (1)AgCl and (1)Pd(CH₃CN)Cl₂ in CH₂Cl₂.

215

216

217 Lastly, we examined the preliminary use of (1)Pd(CH₃CN)Cl₂ in mediating catalytic C-N

218 bond formation. To demonstrate utility, we selected a representative reaction between 2-

219 chloropyrimidine and 1-piperonylpiperazine to form 2-[4-(1,3-benzodioxol-5-ylmethyl)-1-

220 piperazinyl]-pyrimidine (piribedil), a candidate therapeutic for treatment of Parkinson's disease.⁵⁸

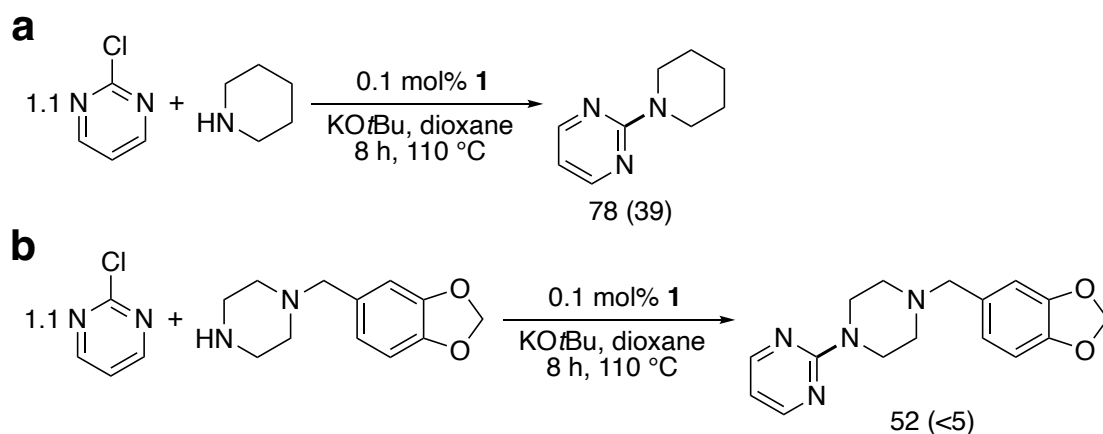
221 Pd catalysts in general⁵⁹ and Pd-NHC complexes^{60,61} in particular have been widely studied for the

222 amination of chloroarenes including halopyrimidines. Both Pd-catalyzed⁶²⁻⁶⁴ and uncatalyzed,

223 direct S_NAr reactions^{62,65} of dialkylamines and 2-chloropyrimidine and its derivatives have been

224 reported, though in the uncatalyzed variants, fluorinated additives or highly polar reaction media

225 are often used. First, we confirmed that (1)Pd(CH₃CN)Cl₂ can mediate the cross-coupling of 2-
226 chloropyrimidine with piperidine itself. Using 0.1 mol% of (1)Pd(CH₃CN)Cl₂, NMR conversion
227 of 96% to the cross-coupled product 2-(1-piperidinyl)pyrimidine was observed (Scheme 3a). The
228 thermal background reaction does occur, but less efficiently (63% NMR conversion). In
229 comparison, no reaction was observed using the meta-halogenated 3-chloropyridine. Using the
230 more highly functionalized amine coupling partner and the same low loading of 0.1 mol%, an
231 isolated yield of 52% of the target complex piribedil was obtained following chromatography
232 (Scheme 3b). In this case, negligible conversion (<5%) was observed in the absence of catalyst.
233



234
235 **Scheme 3.** Synthesis of 2-(1-piperidinyl)pyrimidine and 2-[4-(1,3-benzodioxol-5-ylmethyl)-1-
236 piperazinyl]-pyrimidine (piribedil) catalyzed by (1)Pd(CH₃CN)Cl₂. Isolated yields (%) of
237 catalyzed reactions are shown, with isolated yields of (uncatalyzed) background reactions given in
238 parentheses.

239
240 The synthesis of piribedil by catalytic alkylation of secondary amines with alcohols has been
241 previously reported with higher isolated yields (54-98%), but often requiring higher catalytic
242 loading (1.25-5%).⁶⁶⁻⁷¹ In comparison, fewer reports of formation of piribedil via C-N cross-

243 coupling of 2-chloropyrimidine using pyridine/NHC supported Pd dichloride precatalysts appear
244 in the literature. Formation of piribedil via reductive aminations in an aqueous nanoreactors has
245 been described, with a higher isolated yield (80%) at much lower levels of Pd (2000 ppm).⁷² A
246 related Pd-NHC/pyridine catalyst was also reported to enable near-quantitative yields (98%), albeit
247 at higher loadings (0.2 mol%).⁶⁰

248

249 CONCLUSIONS

250 In conclusion, we have developed a novel phenanthridine-tethered NHC ligand (**1**) and explored
251 its coordination chemistry with late transition metals such as Ag(I) and Pd(II). In the solid-state,
252 the NHC unit of **1** unequivocally coordinates to both transition metals, with the phenanthridinyl
253 arm remaining pendent. The uncoordinated nature of the tethered *N*-heterocycle could further be
254 seen in the weak fluorescence of (**1**)AgCl. The palladium complex (**1**)Pd(CH₃CN)Cl₂ proved a
255 competent precatalyst for a C-N bond forming reaction to form piribedil at a low catalyst loading.
256 Exploration of the scope of these types of reaction and the potential exploitation of bifunctional
257 reactivity arising from the Brønsted basic, pendent phenanthridine is currently underway.

258

259 Experimental Details

260 Unless otherwise stated, all air-sensitive manipulations were carried out inside an inert-atmosphere
261 glove box (N₂) or using standard Schlenk techniques (Ar). 9-fluorenone, POCl₃, POBr₃ (Fisher
262 Scientific), silver oxide and 2,4,6-trimethylaniline (Sigma Aldrich) were purchased from
263 commercial suppliers as reagent grade or better and used as received. 1-(2,4,6-trimethylphenyl)-
264 1*H*-imidazole,⁷³ (COD)PdCl₂,⁷⁴ 6-(5*H*)-phenanthridinone³⁵ and 6-chlorophenanthridine³⁴ were
265 synthesized following published procedures. Organic solvents were dried over appropriate

266 reagents and deoxygenated prior to use. NMR spectra were recorded on a Bruker Avance 300 MHz
267 or Bruker Avance-III 500 MHz spectrometer as noted. High-resolution mass spectra were collected
268 using a Bruker microOTOF-QIII. Absorbance and emission spectra were collected on a Cary 5000
269 UV-Vis NIR spectrophotometer and a PTI QM30 fluorimeter (3 nm slit widths, $\lambda_{\text{exc}} = 310$ nm).
270 Solutions were prepared under ambient, oxygen saturated conditions in CH_2Cl_2 in 10×10 mm²
271 quartz cuvettes. Fluorescence quantum yields (Φ_f) were measured against a quinine sulfate
272 standard, employing the following equation $\Phi_S = \Phi_R \frac{A_R I_S n_S^2}{A_S I_R n_R^2}$, where Φ_R is the reference quantum
273 yield, I is the integrated emission peak, and A is the absorbance at the excitation wavelength (λ_{exc}
274 = 310 nm), and n is the solvent refractive index.⁷⁵

275 **Synthesis of 6-bromophenanthridine:** A 100 mL Schlenk flask was charged with
276 phenanthridinone (1.17 g, 6.0 mmol) and POBr_3 (2.87 g, 10.0 mmol). This mixture was sealed and
277 heated with stirring for 4 h in an oil bath set to 150 °C, then cooled to ambient temperature and
278 left to sit overnight. The mixture was subsequently quenched with a saturated $\text{Na}_2\text{CO}_{3(\text{aq})}$ solution
279 (250 mL), followed by a saturated $\text{NaOH}_{(\text{aq})}$ solution until all the product could be transferred into
280 a large beaker. The resulting suspension was then extracted with CH_2Cl_2 (3×250 mL) and the
281 organic fraction collected using a separatory funnel. This solution was dried over Na_2SO_4 , filtered
282 and dried under reduced pressure to leave a dark brown solid. Yield = 1.31 g (84%). ¹H NMR
283 (CDCl_3 , 300 MHz, 22°C): δ 8.61-8.53 (overlapped m, 2H; C_{ArH}), 8.46 (m, $J_{\text{HH}} = 9$ Hz, 1H; C_{ArH}),
284 8.13-8.10 (m, 1H; C_{ArH}), 7.93-7.88 (m, 1H; C_{ArH}), 7.79-7.67 ppm (overlapped m, 3H; C_{ArH}).

285 **Synthesis of 1•HCl:** The procedure was adapted from the reported synthesis of a quinolinyl-
286 tethered analog.¹⁶ A 50 mL Teflon-stoppered flask was charged with 6-chlorophenanthridine (0.17
287 g, 0.8 mmol), (*N*-mesityl)imidazolium (0.19 g, 1.0 mmol) and toluene (10 mL). The mixture was

288 heated with stirring for 48 h in an oil bath set to 130 °C. The resulting suspension was cooled to
289 room temperature, filtered and the collected solid washed with diethylether (3 × 5 mL) leaving a
290 white solid. Yield = 0.25 g (81%). ¹H NMR (DMSO-d₆, 300 MHz, 22 °C): δ 10.28 (s, 1H; NCHN),
291 9.14 (d, *J*_{HH} = 8.4 Hz, 1H; ^{phen}C_{Ar}H), 9.05-9.02 (m, 1H; ^{phen}C_{Ar}H), 8.79 (m, 1H; ^{imidazole}C_{Ar}H), 8.39
292 (m, 1H; ^{imidazole}C_{Ar}H), 8.26-8.18 (overlapped m, 2H; ^{phen}C_{Ar}H), 8.07-7.96 (overlapped m, 4H;
293 ^{phen}C_{Ar}H), 7.23 (s, 2H; ^{mesityl}C_{Ar}H), 2.38 (s, 3H; ^{para,mesityl}CH₃), 2.23 ppm (s, 6H; ^{ortho,mesityl}CH₃).
294 ¹³C {¹H} NMR (DMSO-d₆, 75 MHz, 22 °C): δ 145.5 (NC_{Ar}HN), 141.2 (^{phen}C=N), 140.6 (C_{Ar}H),
295 139.0 (C_{Ar}), 134.8 (C_{Ar}H), 134.3 (C_{Ar}), 133.1 (C_{Ar}), 131.1 (C_{Ar}H), 130.4 (C_{Ar}H), 129.7 (C_{Ar}), 129.5
296 (C_{Ar}H), 129.4 (C_{Ar}H), 125.2 (C_{Ar}), 124.7 (C_{Ar}H), 124.5 (C_{Ar}H), 124.4 (C_{Ar}), 123.5 (C_{Ar}), 123.4
297 (C_{Ar}H), 120.2 (C_{Ar}), 20.7 (^{para,mesityl}CH₃), 17.2 ppm (^{ortho,mesityl}CH₃).

298 **Synthesis of 1•HBr:** The same synthetic procedure was followed as for the preparation of 1•HCl
299 using: 6-bromophenanthridine (0.20 g, 0.8 mmol), (*N*-mesityl)imidazolium (0.19 g, 1.0 mmol),
300 toluene (10 mL). Light beige solid. Yield = 0.29 g (85%). ¹H NMR (CDCl₃, 300 MHz, 22°C): δ
301 10.62 (s, 1H; NCHN), 8.78 (m, 1H; ^{imidazole}C_{Ar}H), 8.69-8.66 (m, 1H; ^{phen}C_{Ar}H), 8.50 (s, 1H;
302 ^{imidazole}C_{Ar}H), 8.32 (m, 1H; ^{phen}C_{Ar}H), 8.18-8.15 (m, 1H; ^{phen}C_{Ar}H), 8.07-7.91 (overlapped m, 3H;
303 ^{phen}C_{Ar}H), 7.87-7.81 (m, 2H; ^{phen}C_{Ar}H), 7.08 (overlapped s, 2H; ^{mesityl}C_{Ar}H), 2.37 (s, 3H;
304 ^{para,mesityl}CH₃), 2.31 ppm (s, 6H; ^{ortho,mesityl}CH₃). ¹³C {¹H} NMR (CDCl₃, 125 MHz, 22 °C): δ 144.6
305 (NC_{Ar}HN), 141.7 (^{phen}C=N), 138.1 (C_{Ar}), 135.7 (C_{Ar}), 134.3 (C_{Ar}H), 133.1 (C_{Ar}), 130.7 (C_{Ar}), 130.3
306 (C_{Ar}), 130.2 (C_{Ar}H), 130.1 (C_{Ar}H), 129.9 (C_{Ar}H), 129.5 (C_{Ar}), 125.3 (C_{Ar}), 125.2 (C_{Ar}H), 125.1
307 (C_{Ar}H), 124.6 (C_{Ar}H), 123.2 (C_{Ar}H), 122.7 (C_{Ar}H), 119.5 (C_{Ar}), 21.3 (^{para,mesityl}CH₃), 18.2 ppm
308 (^{ortho,mesityl}CH₃).

309 **Synthesis of 1•HPF₆:** This has been synthesized following the modified method of published
310 procedure.¹⁶ In a 20 mL scintillation vial, 1•HCl (0.40 g, 1.0 mmol) was dissolved in 5 mL of a

311 9:1 ratio of water and methanol. Sodium hexafluorophosphate (0.84 g, 5.0 mmol) was added and
312 the mixture stirred for 2 d under ambient conditions, during which time a precipitate formed. The
313 precipitated solid was isolated by filtration, washed with diethylether (3 × 5 mL) and dried under
314 vacuum to yield a white solid. Yield = 0.46 g (91%). ¹H NMR (CD₃CN, 300 MHz, 22 °C): δ 9.33
315 (s, 1H; NCHN), 8.96-8.93 (m, 1H; imidazoleC_{Ar}H), 8.85-8.82 (m, 1H; phenC_{Ar}H), 8.31 (m, 1H;
316 imidazoleC_{Ar}H), 8.20-8.06 (overlapped m, 3H; phenC_{Ar}H), 7.95-7.91 (overlapped m, 3H; phenC_{Ar}H),
317 7.83 (m, 1H; phenC_{Ar}H), 7.20 (m, 2H; mesitylC_{Ar}H), 2.39 (s, 3H; para,mesitylCH₃), 2.23 ppm (s, 6H;
318 ortho,mesitylCH₃). ¹³C{¹H} NMR (CD₃CN, 75 MHz, 22 °C): δ 146.1 (NC_{Ar}HN), 142.7 (phenC=N),
319 138.6 (C_{Ar}), 136.4 (C_{Ar}), 135.7 (C_{Ar}H), 134.0 (C_{Ar}), 131.8 (C_{Ar}), 131.3 (C_{Ar}H), 130.9 (C_{Ar}H),
320 130.6 (C_{Ar}H), 130.5 (C_{Ar}H), 130.2 (C_{Ar}H), 126.0 (C_{Ar}), 125.7 (C_{Ar}H), 125.5 (C_{Ar}H), 125.2 (C_{Ar}H),
321 124.4 (C_{Ar}H), 124.0 (C_{Ar}H), 121.1 (C_{Ar}), 21.2 (para,mesitylCH₃), 17.7 ppm (ortho,mesitylCH₃). ¹⁹F NMR
322 (282 MHz, 22°C, CD₃CN): -72.8 ppm (d, ¹J_{PF} = 707 Hz). ³¹P{¹H} (121 MHz, 22°C, CD₃CN): -
323 144.6 ppm (sep).

324 **Synthesis of (1)AgCl:** Light sensitive precautions were taken for this reaction. A 50 mL flask was
325 charged with **1**•HCl (0.10 g, 0.25 mmol), Ag₂O (0.03 g, 0.13 mmol) and acetonitrile (10 mL). The
326 mixture was heated in an oil bath set to 50°C, with stirring, for 16 h. The resulting suspension was
327 cooled to room temperature, filtered through celite and the volatiles of the collected filtrate
328 removed under reduced pressure. The remaining solid was washed with diethylether (3 × 20 mL)
329 and then dichloromethane added until dissolved. The dichloromethane extract was concentrated to
330 half of the total volume and precipitated with slow addition of diethylether. The suspension was
331 filtered, a white solid was collected and dried under vacuum. Yield = 0.03 g (22%) ¹H NMR
332 (CDCl₃, 300 MHz, 22°C): δ 8.77 (m, J_{HH} = 8.8 Hz, 1H; phenC_{Ar}H), 8.68-8.65 (m, 1H; imidazoleC_{Ar}H),
333 8.24-8.21 (m, 1H; imidazoleC_{Ar}H), 8.00-7.95 (m, 1H; phenC_{Ar}H), 7.88-7.72 (overlapped m, 5H;

334 $^{\text{phen}}\text{C}_{\text{Ar}}\text{H}$), 7.24 (s, 1H; $^{\text{phen}}\text{C}_{\text{Ar}}\text{H}$), 7.03 (s, 2H; $^{\text{mesityl}}\text{C}_{\text{Ar}}\text{H}$), 2.36 (s, 3H; $^{\text{para,mesityl}}\text{CH}_3$), 2.20 ppm (s,
335 6H; $^{\text{ortho,mesityl}}\text{CH}_3$). $^{13}\text{C}\{^1\text{H}\}$ NMR (CD_3CN , 75 MHz, 22 °C): δ 142.9 ($^{\text{phen}}\text{C}=\text{N}$), 140.6 (C_{Ar}), 136.5
336 (C_{Ar}), 136.1 ($\text{C}_{\text{Ar}}\text{H}$), 135.8 ($\text{C}_{\text{Ar}}\text{H}$), 133.2 (C_{Ar}), 130.7 (C_{Ar}), 130.6 (C_{Ar}), 130.1 (C_{Ar}), 129.6 (C_{Ar}),
337 129.5 ($\text{C}_{\text{Ar}}\text{H}$), 126.4 ($\text{C}_{\text{Ar}}\text{H}$), 125.5 (C_{Ar}), 124.3 (C_{Ar}), 124.1 ($\text{C}_{\text{Ar}}\text{H}$), 124.0 ($\text{C}_{\text{Ar}}\text{H}$), 123.8 ($\text{C}_{\text{Ar}}\text{H}$),
338 122.7 ($\text{C}_{\text{Ar}}\text{H}$), 21.2 ($^{\text{para,mesityl}}\text{CH}_3$), 17.9 ppm ($^{\text{ortho,mesityl}}\text{CH}_3$). The carbene ^{13}C resonance and one
339 C_{Ar} peak could not be resolved. HRMS (ESI) calculated for $\text{C}_{50}\text{H}_{42}\text{N}_6\text{Ag}^+$, M^+ : 835.2523. Found:
340 835.2555 (M^+). UV-Vis (CH_2Cl_2 , 22 °C): 297 (6 650), 308 (shoulder), 323 (shoulder), 336 (2 650),
341 352 nm (2 180 $\text{M}^{-1}\text{cm}^{-1}$).

342 **Synthesis of (1)Pd(CH₃CN)Cl₂:** Light sensitive precautions were taken for this reaction. **1**•HCl
343 (0.10 g, 0.25 mmol) and Ag₂O (0.03 g, 0.13 mmol) were combined in a 50 mL Schlenk flask under
344 Ar with acetonitrile (3 mL) and stirred in an oil bath set to 50 °C for 12 h. The consumption of
345 Ag₂O was visually monitored, with formation of a grey solution. After 12 h, a solution of
346 (COD)PdCl₂ (0.07 g, 0.25 mmol) in acetonitrile (2 mL) was added to the mixture and stirring
347 continued for an additional 12 h at the same temperature. The resulting yellow solution was filtered
348 and pumped to dryness under vacuum leaving a solid which was purified using column
349 chromatography (silica, 1:1 CH₃CN:diethylether as eluent). Light yellow solid. Yield = 0.05 g
350 (37%). ^1H NMR (CDCl_3 , 300 MHz, 22°C): δ 8.75-8.73 (m, $J_{\text{HH}} = 10$ Hz, 1H; $^{\text{phen}}\text{C}_{\text{Ar}}\text{H}$), 8.67-8.64
351 (d, 1H; $^{\text{imidazole}}\text{C}_{\text{Ar}}\text{H}$), 8.45-8.31 (overlapped m, 2H; $^{\text{phen}}\text{C}_{\text{Ar}}\text{H}$ and $^{\text{imidazole}}\text{C}_{\text{Ar}}\text{H}$), 7.98-7.93 (m, 1H;
352 $^{\text{phen}}\text{C}_{\text{Ar}}\text{H}$), 7.84-7.73 (m, 3H; $^{\text{phen}}\text{C}_{\text{Ar}}\text{H}$), 7.70-7.69 (m, 1H; $^{\text{phen}}\text{CH}$), 7.15-7.12 (m, 1H; $^{\text{phen}}\text{C}_{\text{Ar}}\text{H}$),
353 7.07 (m, 2H; $^{\text{mesityl}}\text{CH}$), 2.42 (s, 6H; $^{\text{ortho,mesityl}}\text{CH}_3$), 2.38 (s, 3H; $^{\text{para,mesityl}}\text{CH}_3$), 2.00 ppm (s, 3H,
354 CH₃CN). Note: A useful $^{13}\text{C}\{^1\text{H}\}$ could not be collected due to low solubility at higher
355 concentrations. HRMS (ESI) calculated for $\text{C}_{25}\text{H}_{21}\text{Cl}_2\text{N}_3\text{Pd}^+$, $\text{M}+\text{nH}$: 542.0213. Found: 542.0204

356 (MH⁺). UV-Vis (CH₂Cl₂, 22 °C): 310 (shoulder), 336 (8 090), 352 (7 670), 367 (6 340 M⁻¹ cm⁻¹),
357 388 nm (shoulder).

358 **Synthesis of 2-(1-Piperidinyl)pyrimidine:** A thick-walled 10 mL side arm Teflon stopper flask
359 was charged with 2-chloropyrimidine (0.03 g, 0.24 mmol), piperidine (0.03 mL, 0.25 mmol) and
360 KO^tBu (0.04 g, 0.36 mmol), followed by (1)Pd(CH₃CN)Cl₂ (0.0002 g, 0.1 mol%) and degassed
361 1,4-dioxane (4 mL). The flask was sealed and heated to reflux behind a blast shield for 8 h. The
362 mixture was then cooled to room temperature and distilled water (5 mL) added. The mixture was
363 extracted with dichloromethane (3 x 5 mL) in a separatory funnel. The organic fraction was
364 collected, dried over Na₂SO₄ and filtered. The resulting solution was dried under vacuum and
365 purified using column chromatography (silica, 1:1 ethyl acetate:hexanes eluent). Yellow oil. Yield
366 = 0.031 g (78%). Note: extended exposure to vacuum led to a significant decrease in the amount
367 of isolated (yield after extended drying = 0.011 g, 28%) suggesting material is volatile at low
368 pressure. Performing the identical reaction but in the absence of (1)Pd(CH₃CN)Cl₂ led to 63%
369 conversion (¹H NMR) and an isolated yield of 0.015 g (39%); yield after extended drying = 0.006
370 g (15%). Spectroscopic data matched that found in the literature.⁶⁵ ¹H NMR (CDCl₃, 300 MHz,
371 22 °C): δ 8.28 (d, ³J_{HH} = 4.7 Hz, 2H), 6.41 (t, ³J_{HH} = 4.7 Hz, 1H), 3.77 (t, 4H), 1.66-1.56 ppm (m,
372 6H). ¹³C{¹H} NMR (CDCl₃, 75 MHz, 22 °C): δ 161.8, 157.8, 109.2, 44.9, 25.9, 25.0 ppm.

373 **Synthesis of Piribedil:** A thick-walled 10 mL side arm Teflon stopper flask was charged with 2-
374 chloropyrimidine (0.03 g, 0.24 mmol), 1-piperonylpiperazine (0.06 g, 0.25 mmol) and KO^tBu
375 (0.04 g, 0.36 mmol), followed by complex (1)Pd(CH₃CN)Cl₂ (0.0002 g, 0.1 mol%) and degassed
376 1,4-dioxane (4 mL). The flask was sealed and heated to reflux behind a blast shield for 8 h. The
377 mixture was then cooled to room temperature and distilled water (5 mL) added. The mixture was
378 extracted with dichloromethane (3 x 5 mL) in a separatory funnel. The organic fraction was

379 collected, dried over Na₂SO₄ and filtered. The resulting solution was dried under vacuum and
380 purified using column chromatography (silica, 4:1 ethyl acetate:hexanes eluent). Off-white solid.
381 Yield = 0.03 g (52%). Spectroscopic data matched that found in the literature.⁷⁶ ¹H NMR (CDCl₃,
382 300 MHz, 22 °C): δ 8.30-8.28 (m, 2H), 6.89 (s, 1H), 6.76 (d, 2H), 6.47 (m, 1H), 5.95 (s, 2H), 3.82
383 (m, 4H), 3.45 (s, 2H), 2.48 ppm (m, 4H). ¹³C{¹H} NMR (CDCl₃, 75 MHz, 22 °C): δ 161.8, 157.8,
384 147.8, 146.8, 131.9, 122.4, 109.9, 109.6, 108.0, 101.1, 63.0, 52.9, 43.8 ppm.

385 **Control Reaction:** An identical procedure as described above was followed, but omitting
386 (1)Pd(CH₃CN)Cl₂. Following workup, but prior to column chromatography, ¹H NMR revealed
387 negligible conversion to product (< 5%), with unreacted 1-piperonylpiperazine representing the
388 vast majority of the isolated material (see Figure S21).

389

390 X-Ray Crystallography

391 For each crystal structure, X-ray data was using collected from a multi-faceted crystal of suitable
392 size and quality selected from a representative sample of crystals of the same habit using an optical
393 microscope. The crystal was mounted on a MiTiGen loop and data collection carried out in a cold
394 stream of nitrogen (150 K; Bruker D8 QUEST ECO; Mo K α radiation). All diffractometer
395 manipulations were carried out using Bruker APEX3 software.⁷⁷ Structure solution and refinement
396 was carried out using XS and XL software, embedded within OLEX2.⁷⁸ The absence of additional
397 symmetry was confirmed using ADDSYM incorporated in the PLATON program.⁷⁹ CCDC Nos.
398 2021640-2021642 contain the supplementary crystallographic data for this paper. The data can be
399 obtained free of charge from The Cambridge Crystallographic Data Centre via
400 www.ccdc.cam.ac.uk/structures.

401 Crystal structure data for **1**•HBr (CCDC 2021640): X-ray quality crystals were grown from a
402 mixture of hexanes and dichloromethane at 298 K. Crystal structure parameters: C₂₆H₂₄BrCl₂N₃
403 529.29 g mol⁻¹, monoclinic, space group *P*2₁/*c*; *a* = 7.4794(2) Å, *b* = 10.7205(3) Å, *c* = 29.9073(8)
404 Å, $\alpha = 90^\circ$, $\beta = 97.1730(10)^\circ$, $\gamma = 90^\circ$, *V* = 2379.29(11) Å³; *Z* = 4, $\rho_{\text{calcd}} = 1.478 \text{ g cm}^{-3}$; crystal
405 dimensions 0.270 x 0.170 x 0.050 mm; $\theta_{\text{max}} = 27.502^\circ$; 46252 reflections, 5452 independent (*R*_{int}
406 = 0.0772), intrinsic phasing; absorption coeff ($\mu = 1.972 \text{ mm}^{-1}$), absorption correction semi-
407 empirical from equivalents (SADABS); refinement (against *F*_o²) with SHELXTL V6.1, 292
408 parameters, 0 restraints, *R*₁ = 0.0499 (*I* > 2 σ) and *wR*₂ = 0.1303 (all data), Goof = 1.030, residual
409 electron density 3.028/−0.555 e Å⁻³.

410 Crystal structure data for **(1)**AgCl (CCDC 2021641): X-ray quality crystals were grown from
411 diffusion of hexanes vapour into dichloromethane at 298 K. Crystal structure parameters:
412 C₂₆H₂₃AgCl₃N₃ 591.69 g mol⁻¹, triclinic, space group *P*-1; *a* = 7.7936(4) Å, *b* = 9.9308(5) Å, *c* =
413 17.0671(9) Å, $\alpha = 82.142(2)^\circ$, $\beta = 86.911(2)^\circ$, $\gamma = 70.260(2)^\circ$, *V* = 1231.60(11) Å³; *Z* = 2, $\rho_{\text{calcd}} =$
414 1.596 g cm⁻³; crystal dimensions 0.124 x 0.087 x 0.050 mm; $\theta_{\text{max}} = 30.497^\circ$; 35741 reflections,
415 7483 independent (*R*_{int} = 0.0405), intrinsic phasing; absorption coeff ($\mu = 0.530 \text{ mm}^{-1}$), absorption
416 correction semi-empirical from equivalents (SADABS); refinement (against *F*_o²) with SHELXTL
417 V6.1, 301 parameters, 0 restraints, *R*₁ = 0.0321 (*I* > 2 σ) and *wR*₂ = 0.0790 (all data), Goof = 1.019,
418 residual electron density 1.27/−0.92 e Å⁻³.

419 Crystal structure data for **(1)**Pd(CH₃CN)Cl₂ (CCDC 2021642): X-ray quality crystals were grown
420 from layering of diethyl ether atop a chloroform solution at -10 °C. Crystal structure parameters:
421 C₂₈H₂₅Cl₅N₄Pd 701.17 g mol⁻¹, monoclinic, space group *P*2₁/*n*; *a* = 11.7288(6) Å, *b* = 19.5348(9)
422 Å, *c* = 12.8998(6) Å, $\alpha = 90^\circ$, $\beta = 104.647(2)^\circ$, $\gamma = 90^\circ$, *V* = 2859.5(2) Å³; *Z* = 4, $\rho_{\text{calcd}} = 1.629$
423 g cm⁻³; crystal dimensions 0.400 x 0.200 x 0.160 mm³; $\theta_{\text{max}} = 30.593^\circ$; 98792 reflections, 8770

424 independent ($R_{\text{int}} = 0.0290$), direct methods; absorption coeff ($\mu = 1.142 \text{ mm}^{-1}$), absorption
425 correction semi-empirical from equivalents (SADABS); refinement (against F_o^2) with SHELXTL
426 V6.1, 350 parameters, 0 restraints, $R_1 = 0.0306$ ($I > 2\sigma$) and $wR_2 = 0.0765$ (all data), Goof = 1.070,
427 residual electron density 0.969/-1.314 e \AA^{-3} .

428

429 **ASSOCIATED CONTENT**

430 **Supporting Information.** Multi-nuclear NMR and HR-MS spectra of all new compounds;
431 solvatochromism plot; crystallographic information files containing all X-ray data.
432 CCDC 2021640-2021642 contain the supplementary crystallographic data for this paper. The data
433 can be obtained free of charge from The Cambridge Crystallographic Data Center via
434 www.ccdc.cam.ac.uk/structures.

435 The following files are available free of charge:

436 Supporting Information File (PDF)

437 Crystallographic Information Files (CIF)

438

439 **AUTHOR INFORMATION**

440 **Corresponding Author**

441 David E. Herbert (david.herbert@umanitoba.ca)

442

443 **ORCIDs**

444 Rajarshi Mondal: 0000-0002-6819-6690

445 Robert J. Ortiz: 0000-0001-9078-765X

446 Jason D. Braun: 0000-0002-5850-8048

447 David E. Herbert: 0000-0001-8190-2468

448

449 **Author Contributions**

450 The manuscript was written through contributions of all authors. All authors have given approval
451 to the final version of the manuscript.

452

453 **Conflicts of Interest**

454 There are no conflicts of interest to declare.

455

456 **ACKNOWLEDGMENTS**

457 The following sources of funding are gratefully acknowledged: Natural Sciences Engineering
458 Research Council of Canada for a Discovery Grant to DEH (RGPIN-2014-03733); the Canadian
459 Foundation for Innovation and Research Manitoba for an award in support of an X-ray
460 diffractometer (CFI #32146); the University of Manitoba for GETS support (RM, JDB) and a
461 Faculty of Science Undergraduate Summer Research Award (RJO).

462

463 REFERENCES

- 464 (1) Hopkinson, M. N.; Richter, C.; Schedler, M.; Glorius, F. An Overview of *N*-Heterocyclic
465 Carbenes. *Nature* **2014**, *510*, 485–496.
- 466 (2) Nelson, D. J.; Nolan, S. P. Quantifying and Understanding the Electronic Properties of *N*-
467 Heterocyclic Carbenes. *Chem. Soc. Rev.* **2013**, *42*, 6723–6753.
- 468 (3) Köhl, O. The Chemistry of Functionalised *N*-Heterocyclic Carbenes. *Chem. Soc. Rev.*
469 **2007**, *36*, 592–607.
- 470 (4) Liddle, S. T.; Edworthy, I. S.; Arnold, P. L. Anionic Tethered *N*-Heterocyclic Carbene
471 Chemistry. *Chem. Soc. Rev.* **2007**, *36*, 1732–1744.
- 472 (5) O, W. W. N.; Lough, A. J.; Morris, R. H. Synthesis and Characterization of Nitrile-
473 Functionalized *N*-Heterocyclic Carbenes and Their Complexes of Silver(I) and
474 Rhodium(I). *Organometallics* **2009**, *28*, 853–862.
- 475 (6) O, W. W. N.; Lough, A. J.; Morris, R. H. Primary Amine Functionalized *N*-Heterocyclic
476 Carbene Complexes of Iridium: Synthesis, Structure, and Catalysis. *Organometallics*
477 **2013**, *32*, 3808–3818.
- 478 (7) Wan, K. Y.; Lough, A. J.; Morris, R. H. Transition Metal Complexes of an (*S,S*)-1,2-
479 Diphenylethylamine-Functionalized *N*-Heterocyclic Carbene: A New Member of the
480 Asymmetric NHC Ligand Family. *Organometallics* **2016**, *35*, 1604–1612.
- 481 (8) O, W. W. N.; Lough, A. J.; Morris, R. H. The Hydrogenation of Molecules with Polar
482 Bonds Catalyzed by a Ruthenium(II) Complex Bearing a Chelating *N*-Heterocyclic
483 Carbene with a Primary Amine Donor. *Chem. Commun.* **2010**, *46*, 8240–8242.
- 484 (9) O, W. W. N.; Morris, R. H. Ester Hydrogenation Catalyzed by a Ruthenium(II) Complex
485 Bearing an *N*-Heterocyclic Carbene Tethered with an NH₂ Group and a DFT Study of the
486 Proposed Bifunctional Mechanism. *ACS Catal.* **2013**, *3*, 32–40.
- 487 (10) O, W. W. N.; Lough, A. J.; Morris, R. H. Transmetalation of a Primary Amino-
488 Functionalized *N*-Heterocyclic Carbene Ligand from an Axially Chiral Square-Planar
489 Nickel(II) Complex to a Ruthenium(II) Precatalyst for the Transfer Hydrogenation of
490 Ketones. *Organometallics* **2009**, *28*, 6755–6761.
- 491 (11) Wan, K. Y.; Roelfes, F.; Lough, A. J.; Hahn, F. E.; Morris, R. H. Iridium and Rhodium
492 Complexes Containing Enantiopure Primary Amine-Tethered *N*-Heterocyclic Carbenes:
493 Synthesis, Characterization, Reactivity, and Catalytic Asymmetric Hydrogenation of
494 Ketones. *Organometallics* **2018**, *37*, 491–504.

- 495 (12) O, W. W. N.; Lough, A. J.; Morris, R. H. Factors Favoring Efficient Bifunctional
496 Catalysis. Study of a Ruthenium(II) Hydrogenation Catalyst Containing an *N*-Heterocyclic
497 Carbene with a Primary Amine Donor. *Organometallics* **2012**, *31*, 2137–2151.
- 498 (13) Ohara, H.; O, W. W. N.; Lough, A. J.; Morris, R. H. Effect of Chelating Ring Size in
499 Catalytic Ketone Hydrogenation: Facile Synthesis of Ruthenium(II) Precatalysts
500 Containing an *N*-Heterocyclic Carbene with a Primary Amine Donor for Ketone
501 Hydrogenation and a DFT Study of Mechanisms. *Dalton Trans.* **2012**, *41*, 8797–8808.
- 502 (14) Warsink, S.; Bosman, S.; Weigand, J. J.; Elsevier, C. J. Rigid Pyridyl Substituted NHC
503 Ligands, Their Pd(0) Complexes and Their Application in Selective Transfer
504 Semihydrogenation of Alkynes. *Appl. Organomet. Chem.* **2011**, *25*, 276–282.
- 505 (15) Bachmann, M.; Suter, D.; Blacque, O.; Venkatesan, K. Tunable and Efficient White Light
506 Phosphorescent Emission Based on Single Component *N*-Heterocyclic Carbene
507 Platinum(II) Complexes. *Inorg. Chem.* **2016**, *55*, 4733–4745.
- 508 (16) Paloque, L.; Hemmert, C.; Valentin, A.; Gornitzka, H. Synthesis, Characterization, and
509 Antileishmanial Activities of Gold(I) Complexes Involving Quinoline Functionalized *N*-
510 Heterocyclic Carbenes. *Eur. J. Med. Chem.* **2015**, *94*, 22–29.
- 511 (17) Peng, H. M.; Webster, R. D.; Li, X. Quinoline-Tethered *N*-Heterocyclic Carbene
512 Complexes of Rhodium and Iridium: Synthesis, Catalysis, and Electrochemical Properties.
513 *Organometallics* **2008**, *27*, 4484–4493.
- 514 (18) Peng, H. M.; Song, G.; Li, Y.; Li, X. Synthesis, Structures, and Solution Dynamics of
515 Palladium Complexes of Quinoline-Functionalized *N*-Heterocyclic Carbenes. *Inorg.*
516 *Chem.* **2008**, *47*, 8031–8043.
- 517 (19) Ye, J.; Chen, W.; Wang, D. Synthesis, Structural Characterization, and Catalytic
518 Behaviour in Heck Coupling of Palladium(II) Complexes Containing Pyrimidine-
519 Functionalized *N*-Heterocyclic Carbenes. *Dalton Trans.* **2008**, 4015–4022.
- 520 (20) Gu, S.; Chen, W. Pincer Complexes of Palladium- and Nickel-Containing 3-Butyl-1-(1,10-
521 phenanthroline-2-yl)imidazolylidene as Efficient Aqueous Sonogashira and Kumada
522 Coupling Reactions. *Organometallics* **2009**, *28*, 909–914.
- 523 (21) Specht, Z. G.; Cortes-Llamas, S. A.; Tran, H. N.; van Niekerk, C. J.; Rancudo, K. T.;
524 Golen, J. A.; Moore, C. E.; Rheingold, A. L.; Dwyer, T. J.; Grotjahn, D. B. Enabling
525 Bifunctionality and Hemilability of *N*-Heteroaryl NHC Complexes. *Chem. - Eur. J.* **2011**,
526 *17*, 6606–6609.
- 527 (22) Schroeter, F.; Cisarova, I.; Soellner, J.; Herdtweck, E.; Strassner, T. Electron-Poor
528 Hemilabile Dicationic Palladium NHC Complexes - Synthesis, Structure and Catalytic
529 Activity. *Dalton Trans.* **2018**, *47*, 16638–16650.

- 530 (23) Warsink, S.; Chang, I.-H.; Weigand, J. J.; Hauwert, P.; Chen, J.-T.; Elsevier, C. J. NHC
531 Ligands with a Secondary Pyrimidyl Donor for Electron-Rich Palladium(0) Complexes.
532 *Organometallics* **2010**, *29*, 4555–4561.
- 533 (24) Mondal, R.; Giesbrecht, P. K.; Herbert, D. E. Nickel(II), Copper(I) and Zinc(II)
534 Complexes Supported by a (4-Diphenylphosphino)Phenanthridine Ligand. *Polyhedron*
535 **2016**, *108*, 156–162.
- 536 (25) Lozada, I. B.; Murray, T.; Herbert, D. E. Monomeric Zinc(II) Amide Complexes
537 Supported by Bidentate, Benzannulated Phenanthridine Amido Ligands. *Polyhedron* **2019**,
538 *161*, 261–267.
- 539 (26) Mandapati, P.; Braun, J. D.; Sidhu, B. K.; Wilson, G.; Herbert, D. E. Catalytic C–H Bond
540 Alkylation of Azoles with Alkyl Halides Mediated by Nickel(II) Complexes of
541 Phenanthridine-Based $N^{\wedge}N^{\wedge}N$ Pincer Ligands. *Organometallics* **2020**, *39*, 1989–1997.
- 542 (27) Braun, J. D.; Lozada, I. B.; Kolodziej, C.; Burda, C.; Newman, K. M. E.; van Lierop, J.;
543 Davis, R. L.; Herbert, D. E. Iron(II) Coordination Complexes with Panchromatic
544 Absorption and Nanosecond Charge-Transfer Excited State Lifetimes. *Nat. Chem.* **2019**,
545 *11*, 1144–1150.
- 546 (28) Fish, R. H.; Tae-Jeong, K.; Stewart, J. L.; Bushweller, J. H.; Rosen, R. K.; Dupon, W. J.
547 Synthesis of Dimetallaazacyclobutenes via Reaction of Polynuclear Heteroaromatic
548 Nitrogen Compounds with Triruthenium Dodecacarbonyl: Reactivity and Structural
549 Elucidation. *Organometallics* **1986**, 2193–2198.
- 550 (29) Rosenberg, E.; Joynal Abedin, M.; Rokhsana, D.; Viale, A.; Dastrù, W.; Gobetto, R.;
551 Milone, L.; Hardcastle, K. Ligand Dependent Structural Changes in the Acid–Base
552 Chemistry of Electron Deficient Benzoheterocycle Triosmium Clusters. *Inorg. Chim. Acta*
553 **2002**, *334*, 343–354.
- 554 (30) Khoshtarkib, Z.; Ebadi, A.; Alizadeh, R.; Ahmadi, R.; Amani, V.
555 Dichloridobis(phenanthridine- $[\kappa]N$)zinc(II). *Acta Crystallographica Section E*, **2009**, *65*,
556 m739–m740.
- 557 (31) Park, G. Y.; Wilson, J. J.; Song, Y.; Lippard, S. J. Phenanthriplatin, a Monofunctional
558 DNA-Binding Platinum Anticancer Drug Candidate with Unusual Potency and Cellular
559 Activity Profile. *Proc. Natl. Acad. Sci.* **2012**, *109*, 11987–11992.
- 560 (32) Choopani Jouybari, H.; Alizadeh, R.; Banisaeed, H.; Amani, V. Synthesis, Luminescence
561 Studies and Structural Characterization of New Co(II) and Cu(II) Complexes Based on
562 Phenanthridine as a Ligand. *Inorg. Chim. Acta* **2020**, *506*, 119553.
- 563 (33) Mondal, R.; Lozada, I. B.; Davis, R. L.; Williams, J. A. G.; Herbert, D. E. Exploiting
564 Synergy between Ligand Design and Counterion Interactions to Boost Room Temperature
565 Phosphorescence from Cu(I) Compounds. *J. Mater. Chem. C* **2019**, *7*, 3772–3778.

- 566 (34) Badger, G. M.; Seidler, J. H.; Thomson, B. Polynuclear Heterocyclic Systems. III. The
567 3,4-Benzacridine-5,10-Dihydro-3,4-Benzacridine Complex. *J. Chem. Soc.* **1951**, 3207–
568 3211.
- 569 (35) Smith, P. A. S. Schmidt Reaction: Experimental Conditions and Mechanism. *J. Am. Chem.*
570 *Soc.* **1948**, *70*, 320–323.
- 571 (36) Mandapati, P.; Giesbrecht, P. K.; Davis, R. L.; Herbert, D. E. Phenanthridine-Containing
572 Pincer-like Amido Complexes of Nickel, Palladium, and Platinum. *Inorg. Chem.* **2017**, *56*,
573 3674–3685.
- 574 (37) Mandapati, P.; Braun, J. D.; Killeen, C.; Davis, R. L.; Williams, J. A. G.; Herbert, D. E.
575 Luminescent Platinum(II) Complexes of *N*[^]*N*[^]*N* Amido Ligands with Benzannulated *N*-
576 Heterocyclic Donor Arms: Quinolines Offer Unexpectedly Deeper Red Phosphorescence
577 than Phenanthridines. *Inorg. Chem.* **2019**, *58*, 14808–14817.
- 578 (38) Lozada, I. B.; Huang, B.; Stilgenbauer, M.; Beach, T.; Qiu, Z.; Zheng, Y.; Herbert, D. E.
579 Monofunctional Platinum(II) Anticancer Complexes Based on Multidentate
580 Phenanthridine-Containing Ligand Frameworks. *Dalton Trans.* **2020**, *49*, 6557–6560.
- 581 (39) Wang, H. M. J.; Lin, I. J. B. Facile Synthesis of Silver(I)–Carbene Complexes. Useful
582 Carbene Transfer Agents. *Organometallics* **1998**, *17*, 972–975.
- 583 (40) Garrison, J. C.; Youngs, W. J. Ag(I) *N*-Heterocyclic Carbene Complexes: Synthesis,
584 Structure, and Application. *Chem. Rev.* **2005**, *105*, 3978–4008.
- 585 (41) Tulloch, A. A. D.; Danopoulos, A. A.; Winston, S.; Kleinhenz, S.; Eastham, G. *N*-
586 Functionalised Heterocyclic Carbene Complexes of Silver. *J. Chem. Soc., Dalton Trans.*
587 **2000**, 4499–4506.
- 588 (42) Lee, H. M.; Chiu, P. L.; Hu, C.-H.; Lai, C.-L.; Chou, Y.-Chun. Synthesis and Structural
589 Characterization of Metal Complexes Based on Pyrazole/Imidazolium Chlorides. *J.*
590 *Organomet. Chem.* **2005**, *690*, 403–414.
- 591 (43) Froseth, M.; Netland, K. A.; Toernroos, K. W.; Dhindsa, A.; Tilset, Mats. Synthesis and
592 Characterization of Novel Pd(II) Complexes with Chelating and Non-Chelating
593 Heterocyclic Iminocarbene Ligands. *Dalton Trans.* **2005**, 1664–1674.
- 594 (44) Bondi, A. Van Der Waals Volumes and Radii. *J. Phys. Chem.* **1964**, *68*, 441–451.
- 595 (45) Ramnial, T.; Abernethy, C. D.; Spicer, M. D.; McKenzie, I. D.; Gay, I. D.; Clyburne, J. A.
596 C. A Monomeric Imidazol-2-ylidene-silver(I) Chloride Complex: Synthesis, Structure,
597 and Solid State ¹⁰⁹Ag and ¹³C CP/MAS NMR Characterization. *Inorg. Chem.* **2003**, *42*,
598 1391–1393.

- 599 (46) De Fremont, P.; Scott, N. M.; Stevens, E. D.; Ramnial, T.; Lightbody, O. C.; Macdonald,
600 C. L. B.; Clyburne, J. A. C.; Abernethy, C. D.; Nolan, S. P. Synthesis of Well-Defined *N*-
601 Heterocyclic Carbene Silver(I) Complexes. *Organometallics* **2005**, *24*, 6301–6309.
- 602 (47) Ren, X.; Wesolek, M.; Braunstein, Pierre. Cu(I), Ag(I), Ni(II), Cr(III) and Ir(I) Complexes
603 with Tritopic N_{imine}CNHCN_{amine} Pincer Ligands and Catalytic Ethylene Oligomerization.
604 *Dalton Trans.* **2019**, *48*, 12895–12909.
- 605 (48) Fulmer, G. R.; Miller, A. J. M.; Sherden, N. H.; Gottlieb, H. E.; Nudelman, A.; Stoltz, B.
606 M.; Bercaw, J. E.; Goldberg, K. I. NMR Chemical Shifts of Trace Impurities: Common
607 Laboratory Solvents, Organics, and Gases in Deuterated Solvents Relevant to the
608 Organometallic Chemist. *Organometallics* **2010**, *29*, 2176–2179.
- 609 (49) Onar, G.; Gurses, C.; Karatas, M. O.; Balcioglu, S.; Akbay, N.; Ozdemir, N.; Ates, B.;
610 Alici, Bulent. Palladium(II) and Ruthenium(II) Complexes of Benzotriazole
611 Functionalized *N*-Heterocyclic Carbenes: Cytotoxicity, Antimicrobial, and DNA
612 Interaction Studies. *J. Organomet. Chem.* **2019**, *886*, 48–56.
- 613 (50) Willans, C. E.; Anderson, K. M.; Paterson, M. J.; Junk, P. C.; Barbour, L. J.; Steed, J. W.
614 *Bis(N-Heterocyclic Carbene) Dipalladium Complexes: Synthesis, Solid-State*
615 *Conformational Studies and Solution Behaviour.* *Eur. J. Inorg. Chem.* **2009**, 2835–2843.
- 616 (51) Liu, Q.-X.; Zhang, W.; Zhao, X.-J.; Zhao, Z.-X.; Shi, M.-C.; Wang, X.-G. NHC Pd^{II}
617 Complex Bearing 1,6-Hexylene Linker: Synthesis and Catalytic Activity in the Suzuki–
618 Miyaura and Heck–Mizoroki Reactions. *Eur. J. Org. Chem.* **2013**, 1253–1261.
- 619 (52) Tato, F.; García-Domínguez, A.; Cárdenas, D. J. Palladium-Catalyzed Acetoxylation of
620 Arenes by Novel Sulfinyl *N*-Heterocyclic Carbene Ligand Complexes. *Organometallics*
621 **2013**, *32*, 7487–7494.
- 622 (53) Mariconda, A.; Grisi, F.; Costabile, C.; Falcone, S.; Bertolasi, V.; Longo, P. Synthesis,
623 Characterization and Catalytic Behaviour of a Palladium Complex Bearing a Hydroxy-
624 Functionalized *N*-Heterocyclic Carbene Ligand. *New J. Chem.* **2014**, *38*, 762–769.
- 625 (54) Dubey, P.; Gupta, S.; Singh, A. K. Trinuclear Complexes of Palladium(II) with
626 Chalcogenated *N*-Heterocyclic Carbenes: Catalysis of Selective Nitrile–Primary Amide
627 Interconversion and Sonogashira Coupling. *Dalton Trans.* **2017**, *46*, 13065–13076.
- 628 (55) Ruamps, M.; Lugan, N.; César, V. A Cationic *N*-Heterocyclic Carbene Containing an
629 Ammonium Moiety. *Organometallics* **2017**, *36*, 1049–1055.
- 630 (56) Mondal, R.; Lozada, I. B.; Davis, R. L.; Williams, J. A. G.; Herbert, D. E. Site-Selective
631 Benzannulation of *N*-Heterocycles in Bidentate Ligands Leads to Blue-Shifted Emission
632 from [(P[^]N)Cu]₂(μ-X)₂ Dimers. *Inorg. Chem.* **2018**, *57*, 4966–4978.

- 633 (57) Gao, J. Monte Carlo Quantum Mechanical-Configuration Interaction and Molecular
634 Mechanics Simulation of Solvent Effects on the $n \rightarrow \pi^*$ Blue Shift of Acetone. *J. Am.*
635 *Chem. Soc.* **1994**, *116*, 9324–9328.
- 636 (58) Millan, M. J. From the Cell to the Clinic: A Comparative Review of the Partial D2/D3
637 Receptor Agonist and A2-Adrenoceptor Antagonist, Piribedil, in the Treatment of
638 Parkinson's Disease. *Pharmacol. Ther.* **2010**, *128*, 229–273.
- 639 (59) Ruiz-Castillo, P.; Buchwald, S. L. Applications of Palladium-Catalyzed C-N Cross-
640 Coupling Reactions. *Chem. Rev.* **2016**, *116*, 12564–12649.
- 641 (60) Huang, F.-D.; Xu, C.; Lu, D.-D.; Shen, D.-S.; Li, T.; Liu, F.-Shou. Pd-PEPPSI-IPentAn
642 Promoted Deactivated Amination of Aryl Chlorides with Amines under Aerobic
643 Conditions. *J. Org. Chem.* **2018**, *83*, 9144–9155.
- 644 (61) Organ, M. G.; Abdel-Hadi, M.; Avola, S.; Dubovyk, I.; Hadei, N.; Kantchev, E. A. B.;
645 O'Brien, C. J.; Sayah, M.; Valente, C. Pd-Catalyzed Aryl Amination Mediated by Well
646 Defined, N-Heterocyclic Carbene (NHC)–Pd Precatalysts, PEPPSI. *Chem. - Eur. J.* **2008**,
647 *14*, 2443–2452.
- 648 (62) Peng, Z.-H.; Journet, M.; Humphrey, G. A Highly Regioselective Amination of 6-Aryl-
649 2,4-Dichloropyrimidine. *Org. Lett.* **2006**, *8*, 395–398.
- 650 (63) Smith, S. M.; Buchwald, S. L. Regioselective 2-Amination of Polychloropyrimidines.
651 *Org. Lett.* **2016**, *18*, 2180–2183.
- 652 (64) Park, N. H.; Vinogradova, E. V.; Surry, D. S.; Buchwald, S. L. Design of New Ligands for
653 the Palladium-Catalyzed Arylation of α -Branched Secondary Amines. *Angew. Chem., Int.*
654 *Ed.* **2015**, *54*, 8259–8262.
- 655 (65) Bhujabal, Y. B.; Vadagaonkar, K. S.; Gholap, A.; Sanghvi, Y. S.; Dandela, R.; Kapdi, A.
656 R. HFIP Promoted Low-Temperature S_NAr of Chloroheteroarenes Using Thiols and
657 Amines. *J. Org. Chem.* **2019**, *84*, 15343–15354.
- 658 (66) Hamid, M. H. S. A.; Williams, J. M. J. Ruthenium-Catalyzed Synthesis of Tertiary
659 Amines from Alcohols. *Tetrahedron Lett.* **2007**, *48*, 8263–8265.
- 660 (67) Shan, S. P.; Dang, T. T.; Seayad, A. M.; Ramalingam, Balamurugan. Reusable Supported
661 Ruthenium Catalysts for the Alkylation of Amines by Using Primary Alcohols.
662 *ChemCatChem* **2014**, *6*, 808–814.
- 663 (68) Quintard, A.; Rodriguez, J. A Step into an Eco-Compatible Future: Iron- and Cobalt-
664 Catalyzed Borrowing Hydrogen Transformation. *ChemSusChem* **2016**, *9*, 28–30.

- 665 (69) Zotova, N.; Roberts, F. J.; Kelsall, G. H.; Jessiman, A. S.; Hellgardt, K.; Hii, K. Kuok.
666 Catalysis in Flow: Au-Catalyzed Alkylation of Amines by Alcohols. *Green Chem.* **2012**,
667 *14*, 226–232.
- 668 (70) Fu, M.-C.; Shang, R.; Cheng, W.-M.; Fu, Y. Boron-Catalyzed *N*-Alkylation of Amines
669 Using Carboxylic Acids. *Angew. Chem., Int. Ed.* **2015**, *54*, 9042–9046.
- 670 (71) Zou, Q.; Wang, C.; Smith, J.; Xue, D.; Xiao, J. Alkylation of Amines with Alcohols and
671 Amines by a Single Catalyst under Mild Conditions. *Chem. - Eur. J.* **2015**, *21*, 9656–9661.
- 672 (72) Thakore, R. R.; Takale, B. S.; Casotti, G.; Gao, E. S.; Jin, H. S.; Lipshutz, B. H.
673 Chemoselective Reductive Aminations in Aqueous Nanoreactors Using Parts per Million
674 Level Pd/C Catalysis. *Org. Lett.* **2020**, *22*, 6324–6329.
- 675 (73) Zhao, Y.; Gilbertson, S. R. Synthesis of Proline-Based *N*-Heterocyclic Carbene Ligands.
676 *Org. Lett.* **2014**, *16*, 1033–1035.
- 677 (74) Tsuji, J. *Palladium Reagents and Catalysts: New Perspectives for the 21st Century*;
678 Hoboken, NJ : Wiley: Hoboken, NJ, 2004.
- 679 (75) Brouwer, A. M. Standards for Photoluminescence Quantum Yield Measurements in
680 Solution (IUPAC Technical Report). *Pure Appl. Chem.* **2011**, *83*, 2213–2228.
- 681 (76) Hamid, M. H. S. A.; Allen, C. L.; Lamb, G. W.; Maxwell, A. C.; Maytum, H. C.; Watson,
682 A. J. A.; Williams, J. M. J. Ruthenium-Catalyzed *N*-Alkylation of Amines and
683 Sulfonamides Using Borrowing Hydrogen Methodology. *J. Am. Chem. Soc.* **2009**, *131*,
684 1766–1774.
- 685 (77) Bruker-AXS. *APEX3 V2016.1-0*; Madison, Wisconsin, USA, 2016.
- 686 (78) Dolomanov, O. V.; Bourhis, L. J.; Gildea, R. J.; Howard, J. A. K.; Puschmann, H.
687 OLEX2: A Complete Structure Solution, Refinement and Analysis Program. *J. Appl.*
688 *Crystallogr.* **2009**, *42*, 339–341.
- 689 (79) Spek, A. L. Structure Validation in Chemical Crystallography. *Acta Cryst.* **2009**, *D65*,
690 148–155.

691